Random Phasing of High-Power Lasers for Uniform Target Acceleration and Plasma-Instability Suppression

Y. Kato, K. Mima, N. Miyanaga, S. Arinaga, Y. Kitagawa, M. Nakatsuka, and C. Yamanaka
Institute of Laser Engineering, Osaka University, Suita, Osaka 565, Japan
(Received 4 October 1983)

By converting a coherent wave to a random-phased wave, the intensity profile on a target becomes easily controllable. Planar as well as spherical targets were irradiated for the first time by the random-phased wave. The targets were uniformly accelerated without being affected by the small-scale intensity nonuniformities. The $\frac{3}{2}$-harmonic emission shows that the plasma waves at $n_c/4$ are only weakly excited in a spherical plasma. Irradiation with short-wavelength, random-phased beams will be suitable for compression.

PACS numbers: 52.50.Jm, 52.25.Ps, 52.35.Mw, 52.40.Db

Direct target irradiation with short-wavelength lasers leads to good coupling efficiency and high ablation pressure with small hot-electron preheat.[1,2] However, the major potential problem in this approach is the irradiation nonuniformity[3] which directly leads to implosion nonuniformity because of the small lateral thermal-smoothing effect with short-wavelength irradiation.[4,5] In this paper we present experimental and theoretical evaluations of the random-phasing technique which we proposed recently[6] as a new approach for achieving uniform irradiation distribution.

So far four schemes have been proposed to control the irradiation nonuniformity on fusion targets. The first scheme is vacuum spatial filtering[7] (VSF). The second scheme is a plasma spatial filter[8] (PSF). These two approaches are not sufficient in controlling the irradiation nonuniformity; there is a lower bound to the cutoff frequency due to pinhole closure in VSF, and controlling the plasma density profile is difficult in PSF. The third scheme is random phasing[6] where a laser beam is first divided into small beamlets having random phases and then superimposed on the target to yield controlled illumination. The fourth scheme which is closely related to random phasing is the induced spatial incoherence developed by Lehmberg and Obenshain[9] in which the interference pattern of multiple laser beamlets is temporally smoothed by use of a broad-bandwidth laser and an echelon grating. In both the third and fourth schemes illumination nonuniformities of long transverse scalelengths, which are dangerous to symmetric compression, are eliminated without loss of laser energy. Although the technique of induced spatial incoherence is very attractive to obtain smooth illumination distribution, temporal spikes in a laser pulse of broad bandwidth will cause nonlinear effects such as self-focusing along the direction of propagation in laser media. Interaction of broad-bandwidth lasers with plasma[10] needs further investigation.

The basic experimental configuration for target irradiation with the random-phased wave (RP wave) is shown in Fig. 1(a). A random-phase plate,[11] which consists of a two-dimensional array of transmitting areas each of which applies a phase shift randomly chosen between 0 and π rad, is placed near the focusing optics. The intensity distribution $I(x,y)$ at (x,y) in the focal plane has an envelope function given by the square of the sinc function. The zeroth-order diffraction square bounded by $x_0,y_0 = \pm\lambda f/d$ contains 82% of the laser energy where d is the length of a unit square of the phase plate. Random intensity fluctuations due to interferences between the waves diffracted from each element of the phase plate are superposed on this envelope function as shown in Fig. 1(b). As a simplified picture, the three-dimensional spatial pattern of the RP wave is composed of randomly distributed bright beamlets which have a typical diameter of $2\lambda f/D$ and a typical length along the propagation direction of $4\lambda(f/D^2)$ (both zero-to-zero intensity), where D is the laser beam diameter.

The root-mean-squared intensity fluctuation $\langle\delta I\rangle$ averaged[9] over the area $(\delta x)^2$, where δx is comparable to the absorption-ablation distance in the ablating plasma, is given by $\langle\delta I\rangle/\langle I\rangle \sim 0.14$ in the experimental condition described later, where $\langle I\rangle$ is the average intensity. In addition, when classical absorption is the dominant absorption process, the intensity fluctuations are averaged along the propagation direction as a result of the finite length of the beamlets. Also, oblique laser beam propagation with respect to the density gradient in spherical plasmas should be quite effective for laterally smoothing small-scale intensity nonuniformities. Therefore we expect that sufficient uniformity is attainable by irradiation of spherical targets with the RP wave of short wavelength, even though the in-

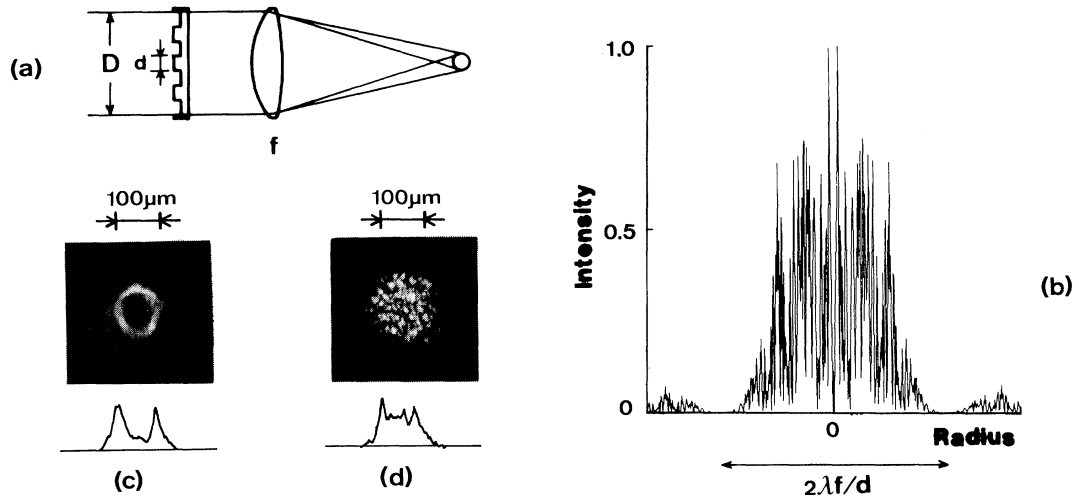

FIG. 1. (a) Typical arrangement of random phasing of the laser beam for uniform target irradiation. A random-phase plate is placed in front of a lens of focal distance f. (b) Calculated intensity distribution of the random-phased wave at the focal plane. (c),(d) Observed intensity distributions of a quasispherical wave and a random-phased wave, respectively. Experimental parameters are given in the text.

terference pattern is stationary in time.[9]

We have fabricated a two-level phase plate where the phase shift is either 0 or π. The experimental parameters were $\lambda = 1.052$ μm, $D = 190$ mm, $d = 7$ mm, and $f = 550$ mm. Figures 1(c) and 1(d) show the intensity distributions 600 μm inside the focal plane without and with the phase plate, respectively. In this example the intensity distribution without the phase plate shows ring structures due to mainly the sinusoidal aberration of $\sim\lambda$ (peak-to-valley) along the radial direction. In this paper we call a spherical wave accompanied with slight aberration a "quasispherical (QS) wave." In contrast the RP wave is insensitive to the intensity nonuniformity and phase aberration, and the overall intensity distribution is easily controllable by the proper selection of the dimensions of the phase plate and the focusing optics.

As in the first experiment, we irradiated solid targets with either the RP wave or the QS wave. Planar or spherical targets were placed inside the focal position (-1300 μm) where the laser beam diameter was approximately 300 μm on the target surface. The laser energy was fixed at 45 J with a pulse width of 350 ps, giving an average laser intensity on the target of $\sim 2\times 10^{14}$ W/cm^2. The intensity of the RP wave was $\sim 25\%$ less than that of the QS wave because of the diffraction and reflection losses of the phase plate. The direction of laser polarization was 22° from the vertical. Target acceleration was observed by backlighting with x rays emitted from a copper plate irradiated by a 350-ps, 140-J, 1.052-μm laser with a time delay of 1 ns. A pinhole camera of 10-μm spatial resolution with 40-μm Be and 10-μm Al filters was used to obtain the backlighting image at 1.1–1.4 keV. The observation direction was normal to the propagation direction and the polarization direction of the laser beam. The time-integrated $3\omega/2$ emission pattern was also recorded normal to the laser beam propagation in a horizontal plane on a Kodak high-speed infrared film whose H-D curve at $3\omega/2$ was calibrated.

The plane target was a flat Mylar of 6 μm thickness and 1.5 mm width. The spherical target was a glass microballoon of ~ 350 μm diameter and 2 μm wall thickness filled with 10 atm D_2. Figures 2(a)–(d) show the x-ray backlighting images of these targets irradiated by one beam of the RP wave and the QS wave. First we examine the data on the plane target [Figs. 2(a) and 2(c)]. The density profile of the rear surface of the accelerated target in Fig. 2(a) is very smooth, and we find none of the small-scale structures contained in the incident wave. There is a possibility that the rear surface has a lower temperature in this case, since the density profile of the accelerated rear surface has a steeper density gradient than that with the QS wave irradiation [Fig. 2(c)] in which the backlighting image of the rear surface has irregularities. In the case of the spherical target, the rear surface of the accelerated target also has a smooth density distribution with the RP wave irradiation. The contour of the accelerated rear surface for the RP wave has a smooth crescent shape, whereas that for the QS wave is flatter and more asymmetric about the optical (laser

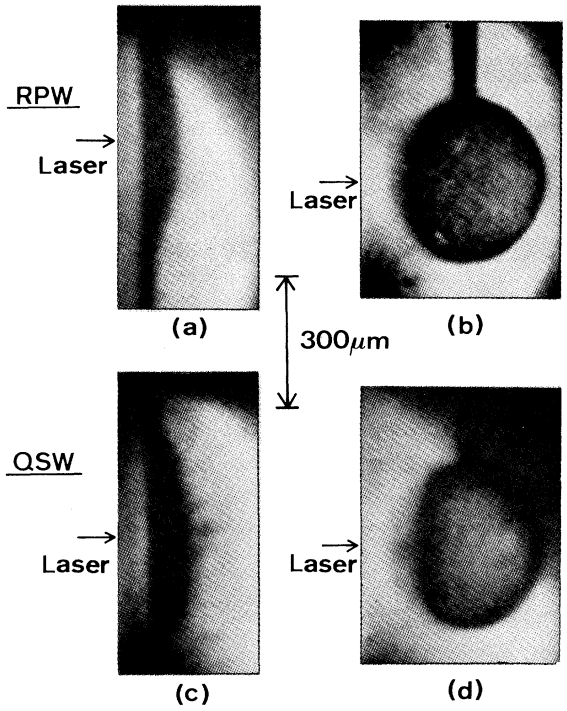

FIG. 2. X-ray backlighting images of (a),(c) a plane target and (b),(d) a spherical target irradiated by (a),(b) the RP wave and (c),(d) the QS wave, respectively.

irradiation) axis.

Figures 3(a)–(d) show the $3\omega/2$ emission patterns and Fig. 3(e) shows their emission distributions in a linear scale calculated from the densitometer traces along the lines marked by arrows in Figs. 3(a)–3(d). In the case of the plane target, the emission distributions resemble the laser intensity distributions on the target. The $3\omega/2$ emission efficiencies are comparable in both cases. The average laser intensity of $\sim 2\times 10^{14}$ W/cm^2 in this experiment is close to the threshold intensity for the two-plasmon decay instability[12] if one assumes a plasma scale length of 30 μm and an electron temperature of 1 keV. We expect then that the instability occurs strongly in the regions where the laser intensity is higher than average and the $\vec{k}$-vector spread of the RP wave could not suppress the instability.

The $3\omega/2$ emission patterns of the spherical target [Figs. 3(b),3(d)] are quite different from the corresponding patterns of the plane target. The emission regions are localized on the laser optical axis, especially with the RP wave irradiation [Fig. 3(b)]. The total emission energy of Fig. 3(b) is $\sim 1\%$ that of Fig. 3(a). In the spherical plasma in comparison to the plane plasma, there will be less two-plasmon decay instability, since the average laser intensity is less and the plasma scale length is shorter.

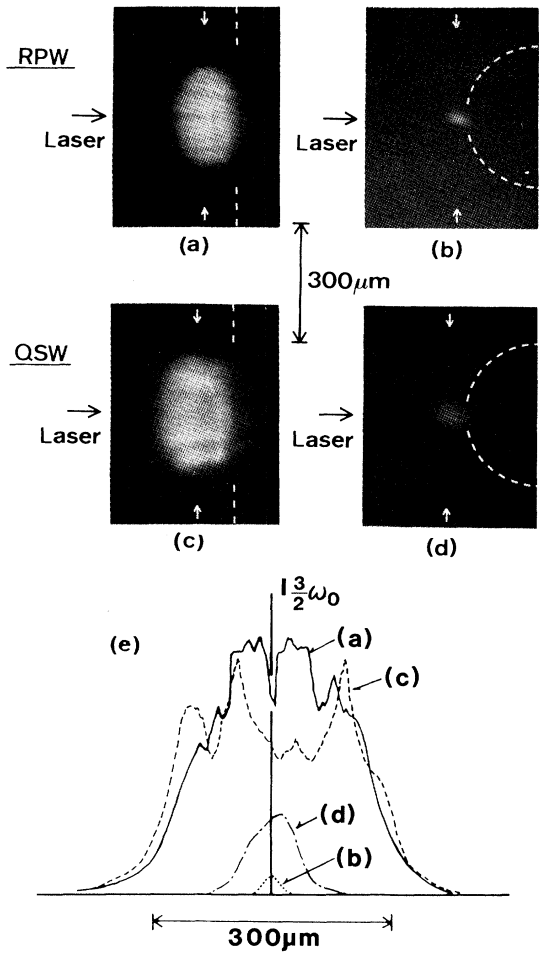

FIG. 3. The $3\omega/2$ emission patterns of (a),(c) a plane target and (b),(d) a spherical target irradiated by (a),(b) the RP wave and (c),(d) the QS wave, respectively. The intensity distributions of (a)–(d) along the lines marked by the arrows are shown in (e). The patterns (a)–(d) are slightly blurred because of reflections in the imaging optics. The vertical direction is inverted (upside down) in (a)–(d).

The RP wave is characterized by broad spatial frequency with phase randomness. When the incident field has a wave-number spread $\Delta k \sim kD/f$, the growth rate of a plasma instability is reduced by $\sim (\Delta k)_{\rm res}/\Delta k$, where $(\Delta k)_{\rm res}$ is the resonance width of the instability in the RP wave. For a filamentation instability

$$(\Delta k)_{\rm res}/k\epsilon^{1/2} \simeq |\delta\epsilon/\epsilon|^{1/2}, \quad (1)$$

where ϵ is the dielectric function of the plasma and $\delta\epsilon$ is the nonlinear part of ϵ. At the laser intensity $I \sim 10^{14}$ W/cm^2, we obtain $\delta\epsilon \sim 10^{-3}$ when T_e equals approximately a few kiloelectronvolts at the

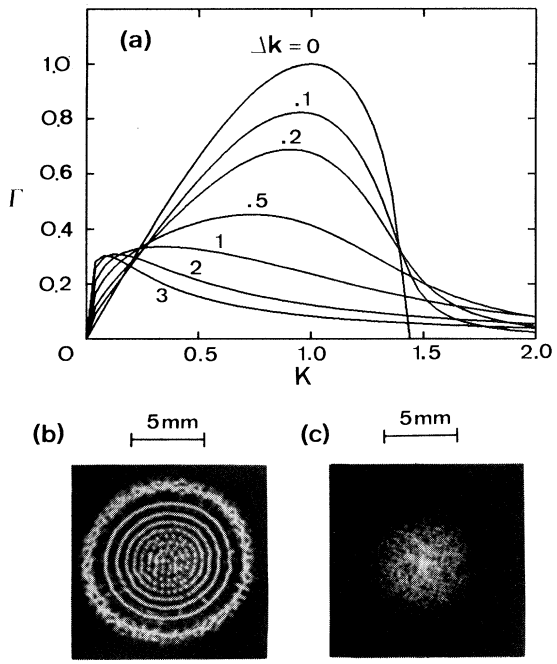

FIG. 4. (a) Dispersion relations for the filamentation instability for various wave-number spreads Δk. End-on view of a laser beam after propagation through liquid carbon disulfide for (b) a collimated coherent wave and (c) a random-phased wave, respectively. The laser wavelength was 1.052 μm and the average laser intensity was 1.6×10^8 W/cm^2 in both cases.

plasma density of $n/n_c = 0.5$. Thus $(\Delta k)_{\rm res}/k \sim 0.03$, and the reduction factor becomes ~ 0.1 for a typical case of $f/D = 3$.

A dispersion relation for the filamentation instability of the RP pump wave has been derived[6] under the Bourret approximation.[13] The resultant dispersion relations for various wave-number spreads, Δk, are shown in Fig. 4(a). The wave number of an unstable mode, K, and the growth rate, Γ, are normalized by the wave number K_m and the growth rate of the fastest growing mode for a coherent pump, respectively, where K_m corresponds to $(\Delta k)_{\rm res}$. We see in Fig. 4(a) that the growth rate is reduced by the factor of $\sim K_m/4\Delta k$ when $\Delta k \gtrsim K_m$.

In a model experiment of the nonlinear propagation of the RP wave in a dielectric medium (carbon disulfide),[14] we found that the self-focusing is indeed suppressed as shown in Fig. 4(c). Namely, the coherent diffraction pattern in Fig. 4(b) breaks up into regularly arranged filaments,[15] but the RP-wave pattern in Fig. 4(c) has no regular-structure characteristics of the periodic breakup as in Fig. 4(b). At $I = 10^8$ W/cm^2, $K_m/2\pi = 30$ cm^{-1} whereas $\Delta k/2\pi \simeq 100$ cm^{-1} in this experiment.

In conclusion, we have shown that irradiation of fusion targets with the random-phased wave results in smooth target acceleration together with the possibility of reduced two-plasmon decay instability in a spherical plasma. Theoretical calculation which is supported by a model experiment reveals that the self-focusing is suppressed when the random-phased wave propagates in a plasma. Direct irradiation of spherical targets with relatively small numbers of short-wavelength, random-phased laser beams is a promising approach in attaining efficient, spherically symmetric compression.

We appreciate critical comments by Dr. R. H. Lehmberg who also sent us Ref. 9 prior to publication. We gratefully thank T. Kanabe, E. Toide, T. Yamada, and T. Otani for experimental cooperation. Participation of ASA Inc. in fabricating the random-phase plate is also acknowledged.

[1]F. Amiranoff, R. Fabbro, E. Fabre, C. Garban, J. Virmont, and M. Weinfeld, Phys. Rev. Lett. **43**, 522 (1979).

[2]W. C. Mead, E. M. Campbell, K. G. Estabrook, R. E. Turner, W. L. Kruer, P. H. Y. Lee, C. E. Max, and M. D. Rosen, Phys. Rev. Lett. **47**, 1289 (1981).

[3]S. E. Bodner, J. Fusion Energy **1**, 221 (1981).

[4]J. H. Gardner and S. E. Bodner, Phys. Rev. Lett. **47**, 1137 (1981).

[5]M. H. Emergy, J. H. Orens, J. H. Gardner, and J. P. Boris, Phys. Rev. Lett. **48**, 253 (1982).

[6]K. Mima and Y. Kato, Institute of Laser Engineering Progress Report on Inertial Fusion Program, May 1982 (unpublished), p. 15; Y. Kato and K. Mima, Appl. Phys. **B29**, 186 (1982).

[7]W. W. Simmons, S. Guch, F. Rainer, and J. E. Murray, IEEE J. Quantum Electron. **11**, 300 (1975).

[8]S. Thomas, K. Moncur, and F. Mayer, KMS Fusion Reports No. KMSF-U459, 1975, No. KMSF-U467, 1976, and No. KMSF-U494, 1976 (unpublished).

[9]R. H. Lehmberg and S. P. Obenschain, Opt. Commun. **46**, 27 (1983).

[10]C. Yamanaka, T. Yamanaka, T. Sasaki, and J. Mizui, Phys. Rev. Lett. **32**, 1038 (1974).

[11]C. B. Burckhardt, Appl. Opt. **9** 695 (1970).

[12]A. B. Langdon and B. F. Lasinski, Lawrence Livermore Report No. UCRL-50021-77, 1978 (unpublished), p. 4-49.

[13]G. Laval, R. Pellat, D. Desme, A. Ramani, M. N. Rosenbluth, and E. A. Williams, Phys. Fluids **20**, 2049 (1977).

[14]Details of this work will be reported elsewhere.

[15]A. J. Campillo, S. L. Shapiro, and B. R. Suydam, Appl. Phys. Lett. **23**, 628 (1973).

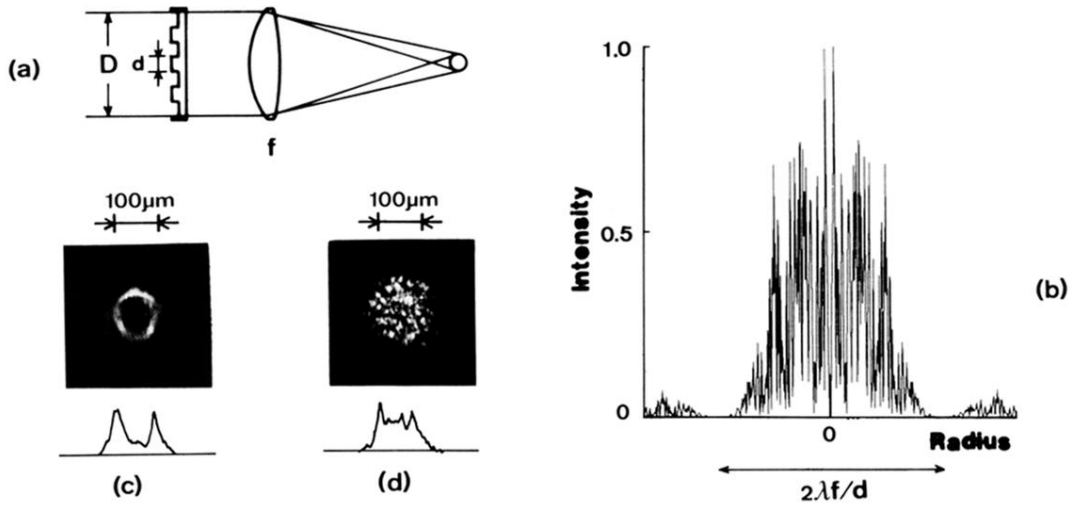

FIG. 1. (a) Typical arrangement of random phasing of the laser beam for uniform target irradiation. A random-phase plate is placed in front of a lens of focal distance f. (b) Calculated intensity distribution of the random-phased wave at the focal plane. (c),(d) Observed intensity distributions of a quasispherical wave and a random-phased wave, respectively. Experimental parameters are given in the text.

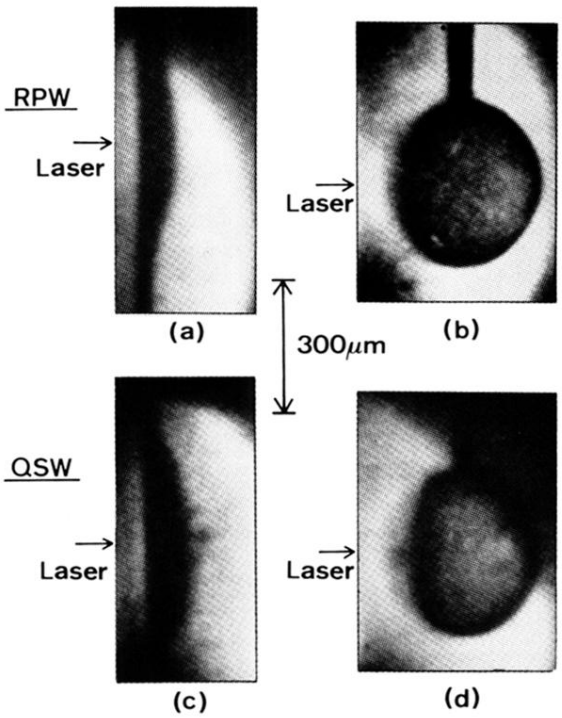

FIG. 2. X-ray backlighting images of (a),(c) a plane target and (b),(d) a spherical target irradiated by (a),(b) the RP wave and (c),(d) the QS wave, respectively.

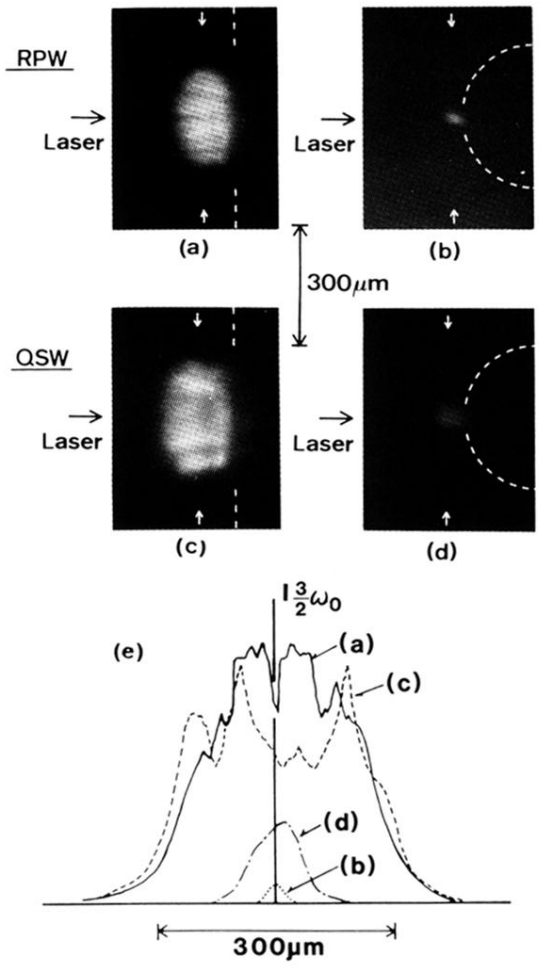

FIG. 3. The $3\omega/2$ emission patterns of (a),(c) a plane target and (b),(d) a spherical target irradiated by (a),(b) the RP wave and (c),(d) the QS wave, respectively. The intensity distributions of (a)–(d) along the lines marked by the arrows are shown in (e). The patterns (a)–(d) are slightly blurred because of reflections in the imaging optics. The vertical direction is inverted (upside down) in (a)–(d).

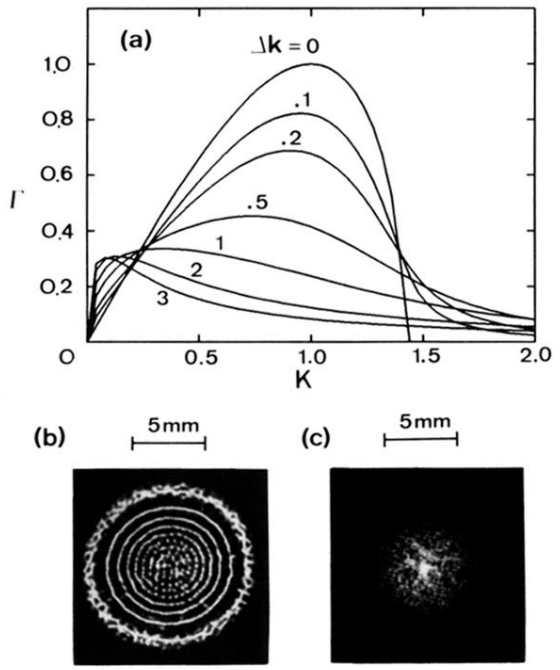

FIG. 4. (a) Dispersion relations for the filamentation instability for various wave-number spreads Δk. End-on view of a laser beam after propagation through liquid carbon disulfide for (b) a collimated coherent wave and (c) a random-phased wave, respectively. The laser wavelength was 1.052 μm and the average laser intensity was 1.6×10^8 W/cm^2 in both cases.